Available online at www.sciencedirect.com
ScienceDirect
Journal of Power Sources 177 (2008) 528–536
JOURNAL OF POWER SOURCES
www.elsevier.com/locate/jpowsour

Dual active material composite cathode structures for Li-ion batteries☆

J.F. Whitacre[a,*], K. Zaghib[b], W.C. West[c], B.V. Ratnakumar[c]

[a] *Carnegie Mellon University, Departments of Materials Science and Engineering/Engineering and Public Policy, Pittsburgh, PA 15213, United States*
[b] *Institut de Recherche d'Hydro-Québec, 1800 Lionel Boulet, Varennes, QC, Canada J3X1S1*
[c] *Jet Propulsion Laboratory, Electrochemical Technologies Group, California Institute of Technology, Pasadena, CA, 91109, United States*

Received 1 November 2007; received in revised form 20 November 2007; accepted 21 November 2007
Available online 10 January 2008

Abstract

The efficacy of composite Li-ion battery cathodes made by mixing active materials that possessed either high-rate capability or high specific energy was examined. The cathode structures studied contained carbon-coated $LiFePO_4$ and either $Li[Li_{0.17}Mn_{0.58}Ni_{0.25}]O_2$ or $LiCoO_2$. These active materials were arranged using three different electrode geometries: fully intermixed, fully separated, or layered. Discharge rate studies, cycle-life evaluation, and electrochemical impedance spectroscopy studies were conducted using coin cell test structures containing Li-metal anodes. Results indicated that electrode configuration was correlated to rate capability and degree of polarization if there was a large differential between the rate capabilities of the two active material species.

Keywords: Mixed active material cathodes; Li Battery; $LiFePO_4$; $LiNiMnO_2$; $LiCoO_2$; Hybrid

1. Introduction

In many applications that rely on Li-ion secondary batteries for energy storage, the nominal duty cycle consists of a long-duration base load (typically to support ancillary or standby functions) punctuated by shorter durations of higher power demand (for events such as physical actuation or communication uplink) [1–3]. In the absence of energy storage technologies that possess both very high specific energy as well as high-rate capability, this type of power profile has led systems designers to select either lower energy density systems that can support high discharge rates, or to specify dual-rate hybrid energy storage systems that use two independent storage devices: one low-rate high energy, the other high-rate low energy [4–6]. This solution leads to increased complexity at the systems level, where separate charge control electronics, packaging, and wiring are needed. We describe below testing done on another possible solution: a dual-rate hybrid battery that is based on two different active cathode materials that are incorporated into the same electrode structure and work in concert.

This approach is not novel, as there have been a number of publications, both in the academic and patent arenas, which describe this idea in a variety of forms. For example, U.S. Patent 7,041,239 by Barker et al. (granted in 2006), "Electrodes comprising mixed active particles" covers a broad range of possible electrode compositions and describes in detail specific cathode active material blends, including mixed $LiMO_2$ layered materials hybridized with $LiMPO_4$ materials [7]. Several groups have also examined mixing spinel $LiMnO_4$ and layered $LiMO_2$ (M = Ni,Co,Mn) materials in the same cathode structure [8–10], while another has examined mixing $LiCoO_2$ and Li_2RuO_3 in a similar fashion [11]. Yet another recent work describes the use of a $LiFePO_4$/$LiCoO_2$ multi-layer cathode structure to increase cell tolerance to overcharge [12]. Still others have examined the efficacy of coating one type of active

☆ All data collected at JPL.
* Corresponding author. Tel.: +1 412 2684458.
E-mail address: whitacre@andrew.cmu.edu (J.F. Whitacre).

0378-7753/$ – see front matter © 2007 Elsevier B.V. All rights reserved.
doi:10.1016/j.jpowsour.2007.11.076

material particle with a disparate active material [13–15]. In the majority of these papers, it is stipulated that the active materials function as though connected in parallel in an equivalent circuit model regardless of how they are assembled in the composite cathode.

Another recent paper offers calculations that indicate high-rate, carbon-coated $LiFePO_4$ can offer a good conductive path, thereby adding to the efficacy of the conductive diluents added [16]. Using this type of active material in a composite system might also result in an increase in electrode conductivity and rate capability.

In creating mixed active material cathodes, there are several parameters that can be manipulated, including: composition, mass ratio, particle morphology, and the physical configuration of functional material within the electrode structure. Here, we offer an examination of the effects of composition, mass ratio and configuration, and use as a test case a combination of high-rate capable carbon-coated $LiFePO_4$ and high specific energy, low-rate capable $Li[Li_{0.17}Mn_{0.58}Ni_{0.25}]O_2$. In some cases, $LiCoO_2$ was also used as an intermediate material in place of the $Li[Li_{0.17}Mn_{0.58}Ni_{0.25}]O_2$.

The $Li[Li_{(1/3-2x/3)}Mn_{(3/2-x/3)}Ni_x]O_2$ cathode system has also reported to be a solid-solution pseudo-binary system, $xLi[Ni_{0.5}Mn_{0.5}]O_2/yLi[Li_{0.33}Mn_{0.67}]O_2$ or alternately as a Li_2MnO_3-stabalized layered structure, $xLi_2MnO_3(1-x)LiMn_yNi_zO_2$, and the Li_2MnO_3 becomes layered $LiMnO_2$ during the first charge step (above 4.5 V) where significant irreversible capacity is observed [17,18]. This system and has been found to have particularly high specific capacity values for the $x=0.5$ and $y=0.5$ (in $xLi[Ni_{0.5}Mn_{0.5}]O_2/yLi[Li_{0.33}Mn_{0.67}]O_2$), and specific capacities of approximately 250 mAh g^{-1} over many cycles have been reported (when charged to 4.8 V), though with relatively low conductivities and corresponding limited rate capability [19–22]. In contrast, the carbon-coated nanoparticulate $LiFePO_4$ material used has been shown to have excellent rate capability, while delivering a specific capacity of over 100 mAh g^{-1} at rates as high as 5*C* [14,23,24].

Dual functional constituent electrode structures based on these materials were made using three different configurations: fully intermixed, fully separated, and layered. The results indicate that the rate capability and specific energy density of the electrode structures depended not only on the composition of the cathode constituents, but also on the way in which they were arranged on the current collector foil. Further testing indicated the cycle-life expectations of this system.

2. Experimental

2.1. Synthesis of the active materials powder

High specific capacity $Li[Li_{0.17}Mn_{0.58}Ni_{0.25}]O_2$, was created using a simple gel combustion synthesis route identical to that reported in the literature [25]. Stoichoimetric quantities of $Mn(CH_3CO_2)_2{\cdot}4H_2O$, $Ni(NO_3)_2{\cdot}6H_2O$, $CH_3CO_2Li{\cdot}2H_2O$ were combined in the proper molar ratio and dissolved in DI H_2O. The mixture was stirred at 100 °C into a viscous gel and subsequently fired at 400 °C overnight, followed by a grinding step, a 500 °C-heating step, another grinding step and a final sintering at 900 °C for 20 h, followed by rapid quenching of the powders on Cu plates. All processing was performed in air. The phase purity of the material was verified using X-ray diffraction. The material was not milled or further modified beyond the original synthesis steps. Fig. 1 shows scanning electron micrographs of this material.

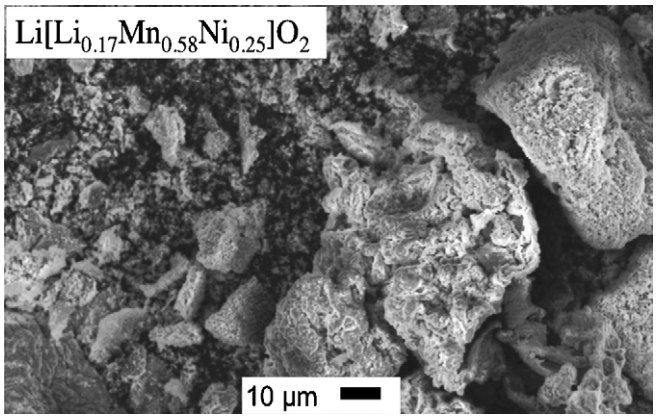

Fig. 1. Scanning electron micrographs of the $Li[Li_{0.17}Mn_{0.58}Ni_{0.25}]O_2$ powder produced at JPL using a gel-fired synthesis route. The larger features consist of small crystalline grains.

High specific power carbon-coated $LiFePO_4$ was synthesized using a hydrothermal process (and subsequent low temperature carbon coating) at Hydroquebec and was identical to that used by Phostech incorporated [23,24,26]. The nominal particle diameter for this material ranged between 50 and 150 nm. The $LiCoO_2$ was acquired from Sony Incorporated, and had particles greater than 1 μm in diameter.

2.2. Composite cathode production

Three classes of cathodes were prepared, as indicated in Fig. 2. The two different active materials were either: (a) completely mixed in a single monolithic electrode, (b) segregated into two different areas, or (c) layered with the $LiFePO_4$ material

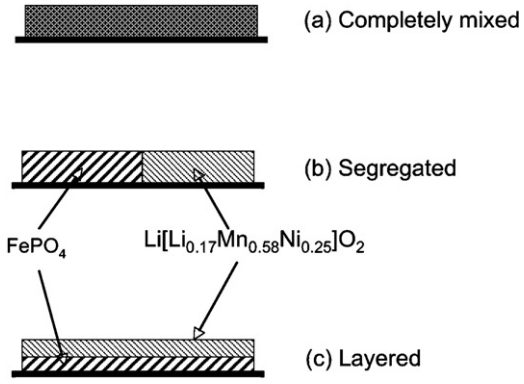

Fig. 2. Schematic of the three different electrode configurations used in this study: (a) completely intermixed, (b) completely segregated (but on the same current collector foil), and (c) layered, with the high-rate $LiFePO_4$ layer in contact with the current collector.

always on the bottom (in contact with the Al current collector). In (a), a single slurry containing both the high-rate carbon-coated $LiFePO_4$ and the high specific energy $Li[Li_{0.17}Mn_{0.58}Ni_{0.25}]O_2$ were mixed in an *N*-methyl pyrrolidinone (NMP) solvent bath with 10 wt.% PVDF binder (fully dissolved in solution) and 10 wt.% carbon black (Shawinigan) conductive diluent. Two mass ratios of $LiFePO_4/Li[Li_{0.17}Mn_{0.58}Ni_{0.25}]O_2$ were used: 1/1 and 3/1. The slurry was spray-deposited onto an Al foil current collector (10 cm × 20 cm) and heated to 140 °C to evaporate the resident NMP. Multiple coatings were used to create a thicker electrode, and the slurry was mixed by hand during and between depositions to encourage full mixing within the solvent bath. Electrodes containing exclusively $LiFePO_4$ or $Li[Li_{0.17}Mn_{0.58}Ni_{0.25}]O_2$ were also spray-deposited and had the same diluent and binder mass fractions as the blended materials. The segregated electrode case, Fig. 2(b), was made from these pure electrodes; 16 mm diameter disks were cut from each, bisected, and placed into the coin cell environment.

For the layered $LiFePO_4/Li[Li_{0.17}Mn_{0.58}Ni_{0.25}]O_2$ cells, both layers were spray-deposited in sequence such that the $LiFePO_4$ was contacting the current collector, with the $Li[Li_{0.17}Mn_{0.58}Ni_{0.25}]O_2$ deposited on top of this. For these samples, NMP based slurries were used for both layers. To avoid solvating the early layers with the solvent in the slurry, the current collector was kept at elevated temperatures, while the rate of spray deposition of fresh slurry was such that it dried completely before affecting preceding layers of cathode material.

For the layered $LiFePO_4/LiCoO_2$ electrodes, a blend of 2 wt.% water soluble binder 6 wt.% conductive carbons (VGCF/Ketjen black), and 92 wt.% C-coated $LiFePO_4$ was first coated onto a C-coated 25 microns thick Al current collector to a thickness of greater than 20 μm. The second layer of $LiCoO_2$ mixed with 2 wt.% VGCF conductive carbon used a 5 wt.% PVDF (Kruha) binder solvated in a non-aqueous solvent (NMP). This layer was slurry cast over the existing $LiFePO_4$ layer and whole structure was heated at 100 °C in the air until dry and then at 100 °C in a vacuum oven for at least 10 h. To maintain porosity and to encourage electrolyte infiltration, the electrodes were not calendared. The total loading of active material in these layered electrodes was 5.77 mg cm^{-2}, and was comprised of 70 wt.% $LiCoO_2$ and 30 wt.% $LiFePO_4$.

2.3. Test cell assembly

All electrodes were vacuum-furnace dried for 24–48 h at ~105 °C and kept in a dry room or glove box environment thereafter. All test cells in this study used Hohsen 2032 coin cell cans (Al clad cathode trays) that were pressed in an Ar filled glove box. Both the Li metal anode and the cathode disks were 16 mm in diameter, and a single layer of Tonen separator was used and was 18 mm in diameter. In all cases the total composite cathode mass for a 16 mm diameter electrode (not including the electrolyte) was between 15 and 20 mg (i.e. 12–16 mg of active material), with thicknesses ranging between 30 and 40 μm. All mass measurements were made using the same microbalance, which was situated inside a dry room (<1% relative humidity). The electrolyte solvent blend was 1:1:1 EC:DMC:DEC with a 1 M $LiBF_4$ salt, a baseline electrode used at JPL [27,28]. Sixteen millimeter diameter Li metal foil was used as an anode material in all cases.

2.4. Electrochemical testing

Galvanostatic cell cycling (with potentiostatic current taper at full charge) was performed using discharge rates from approximately *C*/20 to 3*C* on all cells. All cells containing $Li[Li_{0.17}Mn_{0.58}Ni_{0.25}]O_2$ were charged to 4.8 V, while the $LiCoO_2$-containing cells were charged to 4.2 V. The discharge cutoff potential was 2.0 V in all cases but the $LiCoO_2$-containing bi-layered cathode, used to a 2.5 V cutoff. The initial capacity of the electrodes was determined using a discharge rate no more aggressive than *C*/10, and the cells were always charged galvanostatically using a ~*C*/10 charge rate followed by a 30 min current fade step. Two to five low-rate formation cycles were performed on all cells. As expected, a significant irreversible capacity loss was observed over the first cycle for those cathodes containing $Li[Li_{0.17}Mn_{0.58}Ni_{0.25}]O_2$ [17,19,20]. Several of the cells were also analyzed using electrochemical impedance spectroscopy (EIS) at different states of charge. For these analyses, the cells were maintained at their prescribed cell potential during a 2-h current taper before the EIS scans were conducted. The frequency range used was 200 kHz to 50 mHz. Measurements were performed using either a PAR 273A potentiostat or a PAR VMP2/Z multi-channel potentiostat/impedance spectrometer (now distributed by Bio-Logic). In all cases, at least two cells of each composition and configuration were made and tested to verify reproducibility.

3. Summary of results

The discharge profiles collected under various rates from cells with cathodes containing either pure $LiFePO_4$ or $Li[Li_{0.17}Mn_{0.58}Ni_{0.25}]O_2$ are shown in Fig. 3. The carbon-coated $LiFePO_4$ active material delivered approximately 155 mAh g^{-1} at a *C*/12 rate and 130 mAh g^{-1} at a 3*C*-rate (Fig. 3(a)). The $Li[Li_{0.17}Mn_{0.58}Ni_{0.25}]O_2$ yielded 230 mAh g^{-1} at a *C*/10 rate, and 120 mAh g^{-1} at a 1.7*C*-rate (Fig. 3(b)). The degree of polarization was much more significant for the $Li[Li_{0.17}Mn_{0.58}Ni_{0.25}]O_2$ cathode compared to the $LiFePO_4$ cathode, a result that is consistent with previous assertions that this particular carbon-coated $LiFePO_4$ is capable of sustaining high-rate discharge currents [14,23].

The performance of the electrodes containing fully mixed $LiFePO_4/Li[Li_{0.17}Mn_{0.58}Ni_{0.25}]O_2$ is shown in Fig. 4. Fig. 4(a) shows the results for when there was an equal mass fraction of each active material type, while Fig. 4(b) indicates the same results for when the relative mass fraction of the materials was 75/25 $LiFePO_4/Li[Li_{0.17}Mn_{0.58}Ni_{0.25}]O_2$. In both cases, the cell becomes significantly polarized at higher discharge rates, while the total delivered capacity decreases commensurately. The 75/25 cell polarized to a greater degree than the electrode with an equal mass fractions of both active materials.

Fig. 5 shows the rate capability of a cell made using segregated $LiFePO_4$ and $Li[Li_{0.17}Mn_{0.58}Ni_{0.25}]O_2$ electrode areas (as

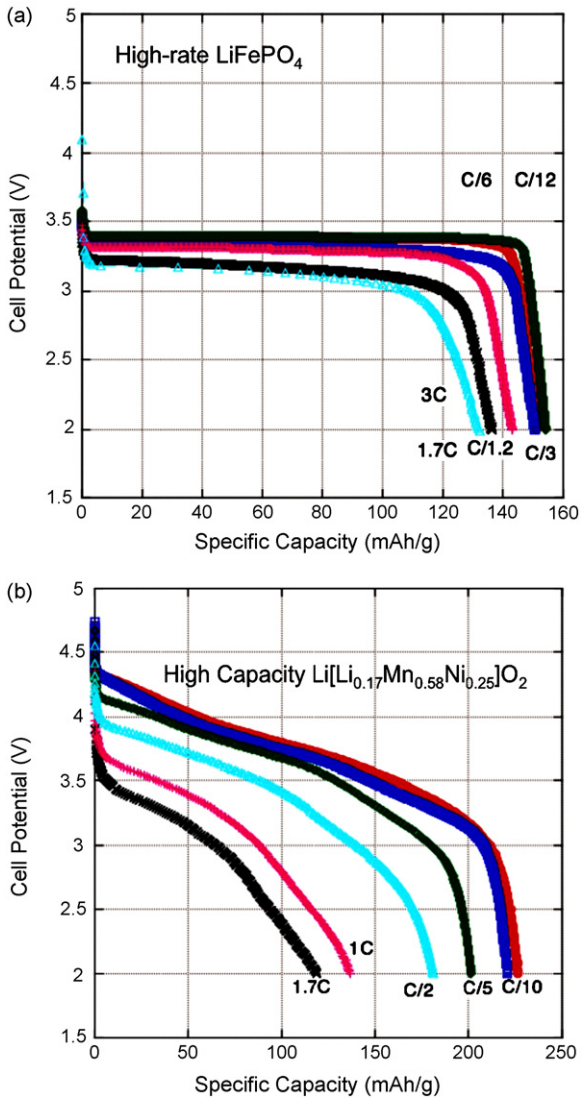

Fig. 3. Discharge rate study of (a) pure carbon-coated $LiFePO_4$, and (b) pure $Li[Li_{0.17}Mn_{0.58}Ni_{0.25}]O_2$. These were collected after several low-rate formation cycles were completed on the cells to encourage electrode SEI stabilization.

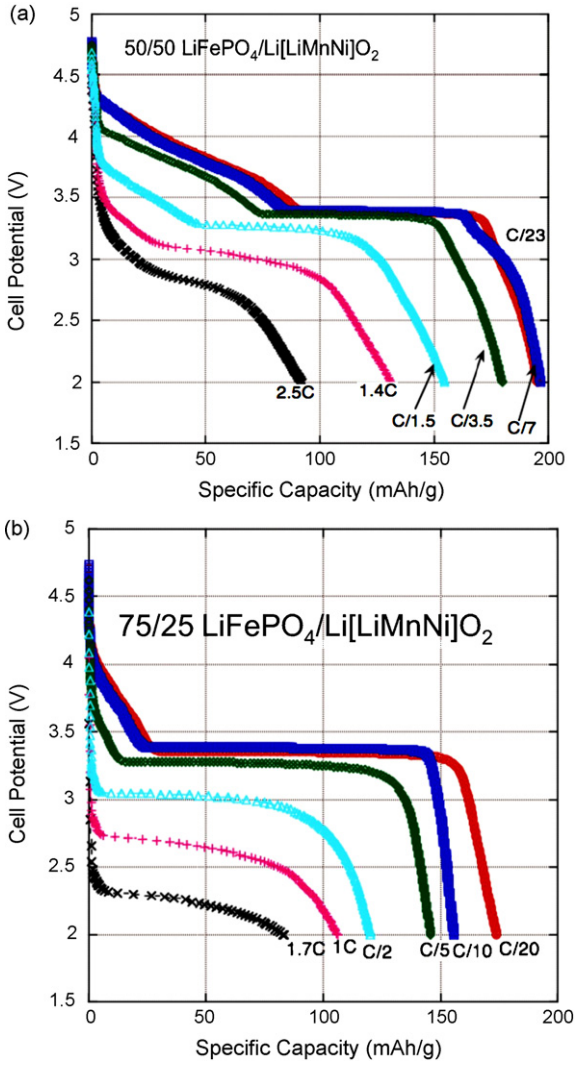

Fig. 4. Discharge rate study of completely intermixed carbon-coated $LiFePO_4$ and $Li[Li_{0.17}Mn_{0.58}Ni_{0.25}]O_2$ in 50/50 and 75/25 wt.% ratios. These were collected after several low-rate formation cycles were completed on the cells to encourage electrode SEI stabilization.

depicted in Fig. 2(b)). Here, the overall structure consisted of 50 wt.% $LiFePO_4$ and 50 wt.% $Li[Li_{0.17}Mn_{0.58}Ni_{0.25}]O_2$. The cathode was able to deliver similar specific capacity values as observed in the fully intermixed cathode cell; however, the observed cell polarization was measurably less under higher rate discharge currents.

Fig. 6 contains data from cells made using the multi-layer electrode configuration (as depicted in Fig. 2(c)). These cells become increasingly polarized under higher loads. Fig. 6(a) contains data from an electrode that had a similar thickness $LiFePO_4$ layer and $Li[Li_{0.17}Mn_{0.58}Ni_{0.25}]O_2$ layer (the total fractional content of the cathode was approximately 50/50 wt.% $LiFePO_4/Li[Li_{0.17}Mn_{0.58}Ni_{0.25}]O_2$. Fig. 6(b) shows similar data for the case where the $LiFePO_4$ was thicker than the $Li[Li_{0.17}Mn_{0.58}Ni_{0.25}]O_2$ layer (where the nominal mass ratio between the two constituents was nominally 75/25 wt.%). In this case, the cell with less overall $Li[Li_{0.17}Mn_{0.58}Ni_{0.25}]O_2$ content became polarized to a lesser extent at progressively higher currents compared to the cell with more $Li[Li_{0.17}Mn_{0.58}Ni_{0.25}]O_2$.

Fig. 7 shows the rate study for the cell containing a 70/30 wt.% $LiCoO_2/LiFePO_4$. At lower rates (lower than *C*/1.2) the higher discharge potential of the $LiCoO_2$ material is distinct. In general, this electrode did not exhibit a significant degree of polarization under higher loads, and the discharge profile was maintained at relatively high potentials. The total specific capacity at low rates is higher than typically expected if it is assumed that $LiCoO_2$ delivers 140 mAh g^{-1}. However, it has been shown recently that pure $LiCoO_2$ can deliver up to 165 mAh g^{-1} (between 4.3 and 3.5 V) under low-rate conditions [29]. The results in Fig. 7 indicate that slightly over 160 mAh g^{-1} was obtained from this $LiCoO_2$ as discharged at low rates, which is within reason.

Fig. 8 contains a reduction of all previous data indicating the delivered specific energy as a function of *C*-rate Fig. 8(a),

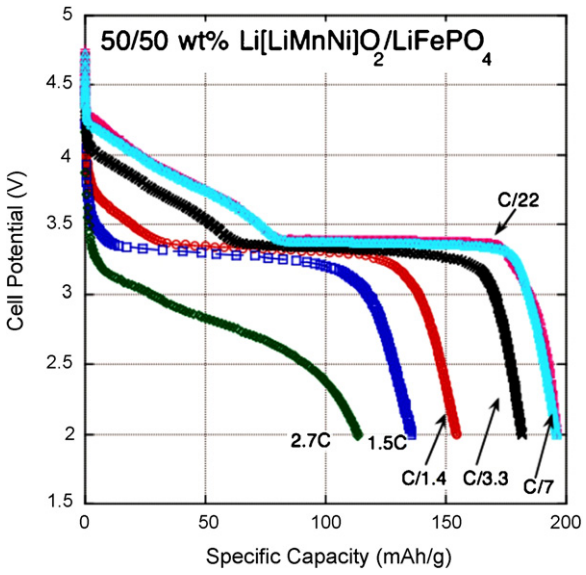

Fig. 5. Discharge rate study of segregated, carbon-coated $LiFePO_4$ and $Li[Li_{0.17}Mn_{0.58}Ni_{0.25}]O_2$ in 50/50 and wt.% ratios. These data were collected after several low-rate formation cycles were completed on the cells to encourage electrode SEI stabilization.

or specific power Fig. 8(b). The average specific power was determined by first calculating the effective discharge potential by dividing the specific energy by the specific capacity. This voltage value was then multiplied by the specific cell current (as normalized to active material mass) to give an average specific power value.

It is important to show how these electrodes might perform under repeated cycling, particularly since the $LiFePO_4$ constituent is fully charged at approximately 3.6 V and must then encounter significant overcharging if the entire cell is charged to a potential of 4.8 V. Fig. 9 shows (a) the first 5 discharges and (b) cycle-life data for one hundred *C*/10 charge/discharge cycles performed on the 50/50 $LiFePO_4$/$Li[Li_{0.17}Mn_{0.58}Ni_{0.25}]O_2$ cell with segregated active areas. There is approximately 10% loss in capacity over 100 cycles, and the nominal columbic efficiency was better than 95% during this test. There does not appear to be any loss in $LiFePO_4$ functionality, and it is likely that some of this capacity fade could be due to an anodic oxidation of the electrolyte as a result of the high charge potentials being used (also consistent with the non-perfect columbic efficiency observed). This effect could be mitigated using different, high electrochemical window tolerant electrolyte solvents.

Electrochemical impedance spectroscopy data are plotted in Fig. 10 for the Li $LiFePO_4$/$Li[Li_{0.17}Mn_{0.58}Ni_{0.25}]O_2$ multi-layer cell (discharge data shown in Fig. 6(b)), There was a substantial variation in electrode impedance (proportional to the low frequency real-axis intercept of the dominant semi-circular feature in the complex plane plot representation) in the $Li[Li_{0.17}Mn_{0.58}Ni_{0.25}]O_2$ containing multi-layer cell as a function of state of charge. Subsequent testing showed that the $Li[Li_{0.17}Mn_{0.58}Ni_{0.25}]O_2$ material was found to undergo a nearly 2-fold increase in overall resistance between 2.6 and 3.6 V, accounting for the majority of the variation in cell impedance during cycling.

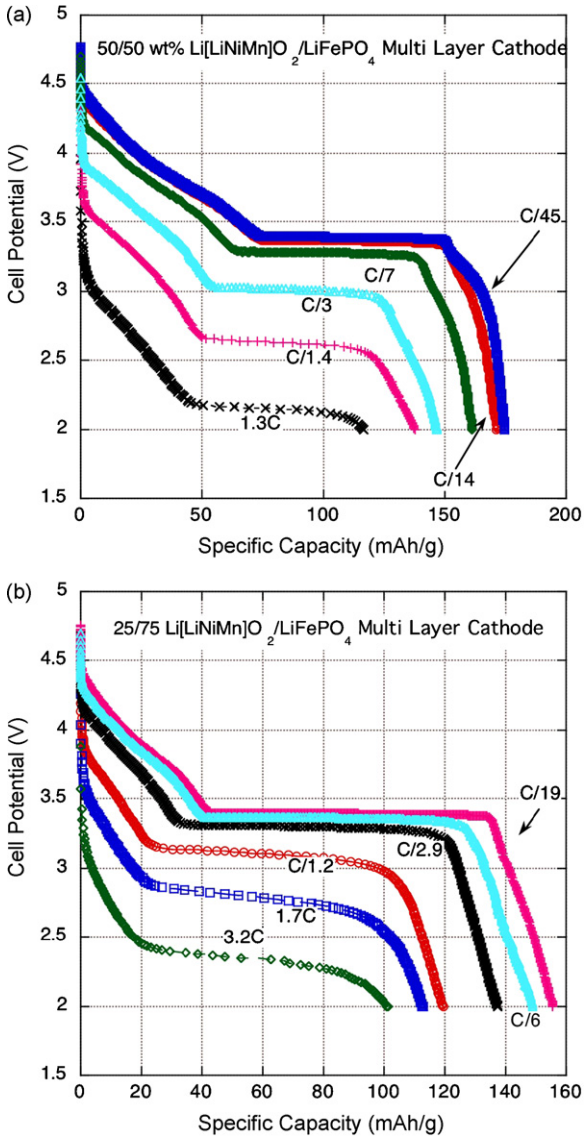

Fig. 6. Discharge rate study of layered carbon-coated $LiFePO_4$ and $Li[Li_{0.17}Mn_{0.58}Ni_{0.25}]O_2$ in (a) 50/50 and (b) 75/25 wt.% ratios. These were collected after several low-rate formation cycles were completed on the cells to encourage electrode SEI stabilization.

4. Discussion

The data show that the manner in which dual active material electrode structures are arranged can significantly affect cell performance if one of the constituents possesses a relatively higher rate capability. In particular, it was less advantageous to completely mix or layer carbon-coated $LiFePO_4$ and $Li[Li_{0.17}Mn_{0.58}Ni_{0.25}]O_2$ powders within a monolithic electrode; this resulted in lower overall energy delivery under similar discharge rates compared to the case when the electrodes were separate but were co-located on the same current collector (case Fig. 2(b)).

In fact, the three different configurations resulted in three distinct discharge profile trends under higher rates. For the sake of this discussion, it is assumed that a characteristic sloping discharge curve starting above 4 V can be attributed to the

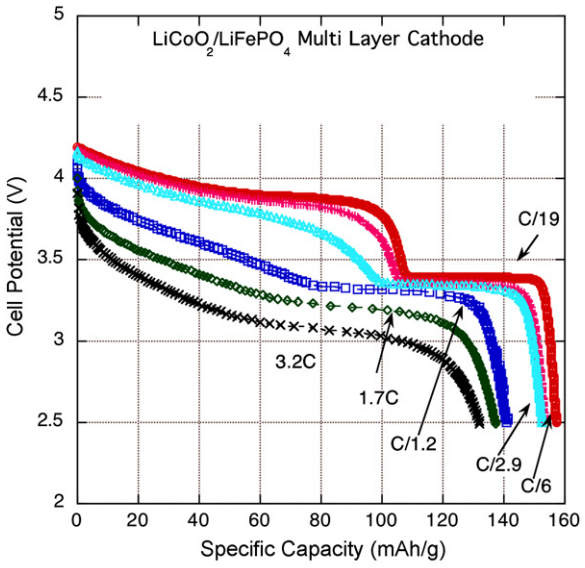

Fig. 7. Discharge rate study of layered carbon-coated $LiFePO_4$ and $LiCoO_2$ in (a) 70/30 wt.% ratio ($LiCoO_2$/$LiFePO_4$). These were collected after several low-rate formation cycles were completed on the cells to encourage electrode SEI stabilization.

$Li[Li_{0.17}Mn_{0.58}Ni_{0.25}]O_2$ content, while the relatively level portion of the curve occurring at less than 3.4 V can be attributed to the carbon-coated $LiFePO_4$. This type of interpretation has been used previously in solid-solution cathodes to associate different electrochemical couples/potential plateaus with different oxidation state constituents [30–32].

When the two active materials were mixed intimately, the $Li[Li_{0.17}Mn_{0.58}Ni_{0.25}]O_2$ contributed proportionally less to the overall cell capacity under higher rates; the higher voltage sloping characteristic discharge curve portion essentially vanished at rates above 1.4*C* and *C*/2 for the 50/50 and 75/25 cases, respectively, as shown in Fig. 4.

For the multi-layer configuration, however, the relative contribution from the $Li[Li_{0.17}Mn_{0.58}Ni_{0.25}]O_2$ did not decrease as much under increasing loads. Here, the cells polarized rapidly, but there was still a large fraction of the discharge curve exhibiting the expected sloping curve associated with the $Li[Li_{0.17}Mn_{0.58}Ni_{0.25}]O_2$ content.

The electrode with segregated active materials behaved differently still, with the $Li[Li_{0.17}Mn_{0.58}Ni_{0.25}]O_2$ contribution to the discharge plateau disappearing at higher rates, this time without significant overall cell polarization. This behavior was similar to that expected from the case when two discrete cells with very different rate capability are connected electronically in parallel.

Fig. 11 is a plot containing relative polarization data for the different cases; here the nominal discharge plateau (as delivered by the by the $LiFePO_4$ constituent) as a function of discharge rate for different compositions and configurations is shown. As described above, the degree of electrode polarization was strongly correlated to electrode configuration when using the low-rate, high-capacity $Li[Li_{0.17}Mn_{0.58}Ni_{0.25}]O_2$ material, with the layered configuration resulting in the highest degree of polarization. However, if the lithium metal oxide con-

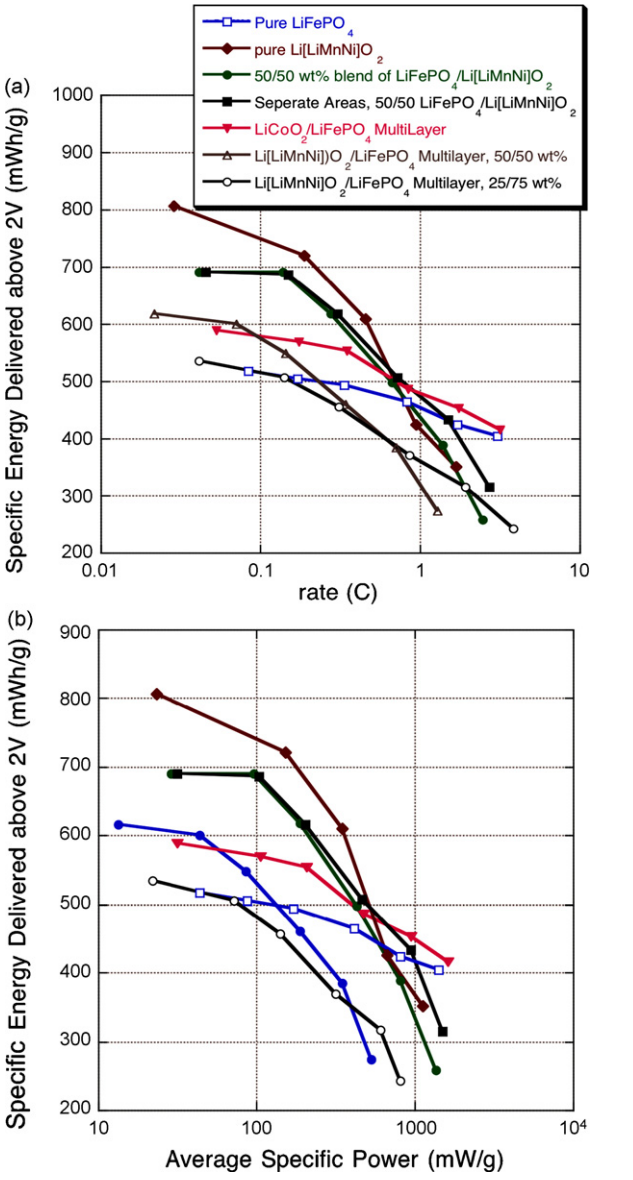

Fig. 8. Rate study data compile: specific energy as a function of (a) discharge rate and (b) average specific discharge power. The average specific discharge power value was determined using an average cell voltage value determined by dividing the integrated specific energy value by the specific capacity, which was then multiplied with the specific current used.

stituent was $LiCoO_2$, a material with higher rate cabability than $Li[Li_{0.17}Mn_{0.58}Ni_{0.25}]O_2$, the layered cell had much improved performance.

Mixing two active materials with disparate rate capabilities into a composite electrode was found to be not equivalent to placing the electrodes in parallel at either an electrode or cell level. Despite the fact that there was significant high surface area conductive diluent present (10 wt.%), and there was a high mass fraction of C-coated $LiFePO_4$, the low-rate capability of the $Li[Li_{0.17}Mn_{0.58}Ni_{0.25}]O_2$ lowered overall electrode specific energy if the materials were mixed intimately or layered on top of each other in a single electrode.

This may be explained as follows. In the case of the physically segregated electrodes, the entire $Li[Li_{0.17}Mn_{0.58}Ni_{0.25}]O_2$

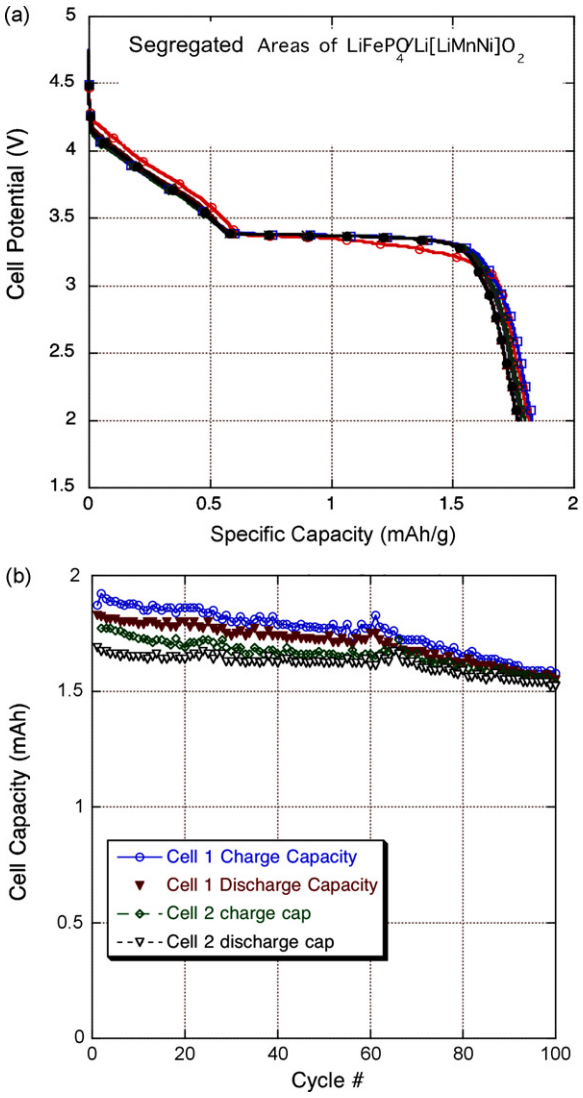

Fig. 9. Cycle-life study conducted on the completely segregated cell (rate study shown in Fig. 5); (a) first 5 discharges at a *C*/10 rate, and (b) charge/discharge capacity as a function of cycle #.

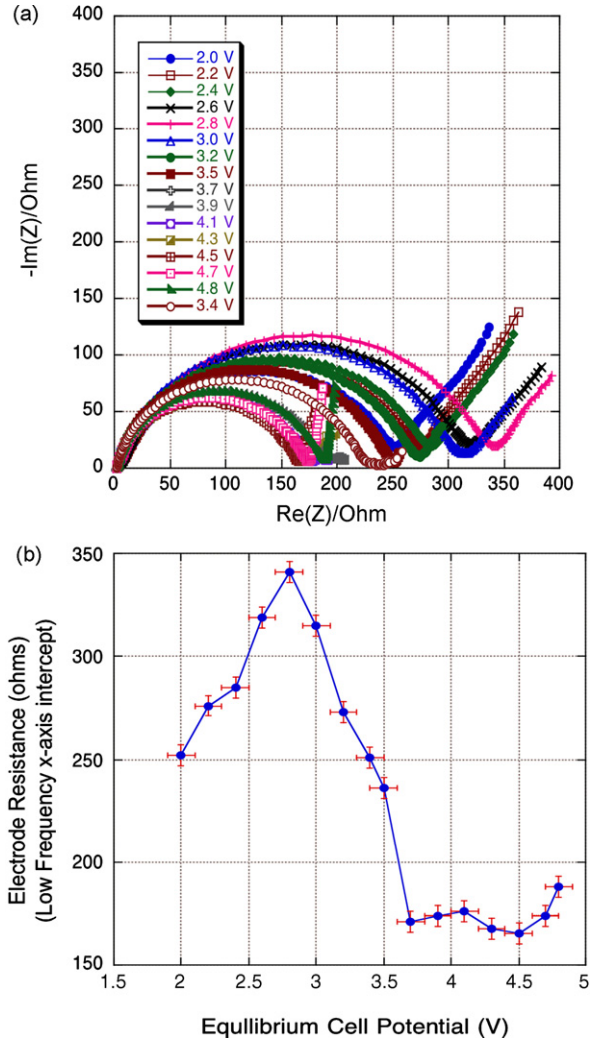

Fig. 10. Electrochemical impedance spectroscopy of the $LiFePO_4$/$Li[Li_{0.17}Mn_{0.58}Ni_{0.25}]O_2$ (50/50 wt.%); (a) Nyquest plot showing the data, and (b) electrode resistance (diameter in ohms of large loop in the Nyquest representation) as a function of state of charge. No significant increase in electrode resistivity was observed above 3.5 V.

electrode could be polarized as a single body under higher discharge rates, thereby driving most current through the $LiFePO_4$ electrode. In this case, it is not requisite that all of the $Li[Li_{0.17}Mn_{0.58}Ni_{0.25}]O_2$ and $LiFePO_4$ active particles be held at the same potential within their separate electrodes.

When the $Li[Li_{0.17}Mn_{0.58}Ni_{0.25}]O_2$ and $LiFePO_4$ were mixed intimately, however, all the particles were forced to be equipotential with their neighbors (as they were in direct electrical contact via the high surface area conductive diluent); this condition resulted in an increased degree of overall electrode polarization, though the higher electronic conductivity of the carbon-coated $LiFePO_4$ material was still able to combat severe polarization to some degree, as it likely offered a direct conductive route through the thickness of the electrode.

The layered material case is more extreme; here both the ionic and electronic conductivities of both of the constituents were manifested, as the carbon-coated $LiFePO_4$ was not present throughout the electrode to aid in electronic conductivity. All cell current was forced to pass through the $Li[Li_{0.17}Mn_{0.58}Ni_{0.25}]O_2$ material. This is consistent with the data that indicated that higher rate discharges on the layered cathode structures displayed significant discharge characteristics from the $Li[Li_{0.17}Mn_{0.58}Ni_{0.25}]O_2$ constituent.

If the carbon-coated $LiFePO_4$ was layered with the higher rate $LiCoO_2$, conditions were improved significantly, an effect also consistent with our interpretation. In fact, Fig. 7 indicates that the specific energy of a layered $LiFePO_4$/$LiCoO_2$ electrode was superior to that of pure $LiFePO_4$ throughout the wide current range examined, though delivered lower specific energies than the $Li[Li_{0.17}Mn_{0.58}Ni_{0.25}]O_2$/$LiFePO_4$ composites (and pure $Li[Li_{0.17}Mn_{0.58}Ni_{0.25}]O_2$) at rates slower than *C*/5.

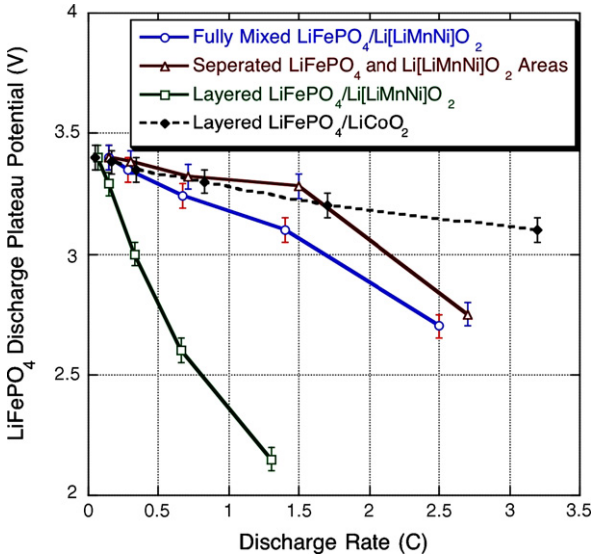

Fig. 11. Nominal $LiFePO_4$ discharge plateau as a function of discharge rate for similar content, differently configured electrodes. Electrode configuration had a strong effect on cell polarization if $Li[Li_{0.17}Mn_{0.58}Ni_{0.25}]O_2$ was present.

The electrochemical impedance spectroscopy data plotted in Fig. 10 show that the overall cell impedance did not increase under higher states of charge, despite the fact that there was a $LiFePO_4$ layer separating the $Li[Li_{0.17}Mn_{0.58}Ni_{0.25}]O_2$ content from the current collector. This result is different from that reported previously, where a layer of $LiFePO_4$ was used as a safety mechanism by virtue of its increased resistivity upon full lithiation. [12] The carbon-coated $LiFePO_4$ used in our study likely possessed much higher overall conductivity than uncoated $LiFePO_4$, even when full de-lithiated, and so the effects observed here were different.

5. Conclusions

The relative merits of using several different composite electrode configurations for dual active material cathodes have been examined. Using constituents with contrasting rate capabilities (high-rate carbon-coated $LiFePO_4$ and high-capacity $Li[Li_{0.17}Mn_{0.58}Ni_{0.25}]O_2$), cathode structures were fabricated that were able to deliver over 700 Wh kg^{-1} at low rates and 300 Wh kg^{-1} at rates as high as 3*C*. If there was a significant conductivity differential between the two active material constituents, it was found that the most promising electrode configuration consisted of segregated active materials contacting a common current collector. This arrangement allowed the high-rate materials to contribute fully under high current loads without suffering the significant polarization effects associated with the low-rate material. This configuration is most similar to putting separate cells made using pure cathodes of the specified materials in parallel at the circuit level, a solution that is less appealing for applications requiring compact energy storage devices and simple charge control electronics.

If the lower specific capacity, higher rate capable $LiCoO_2$ was used instead of $Li[Li_{0.17}Mn_{0.58}Ni_{0.25}]O_2$ in the layered configuration, however, a cathode was made that out-performed electrodes based on pure carbon-coated $LiFePO_4$ for discharge rates ranging from *C*/20 to 5*C* (and likely beyond). This is an important result because it indicates that a $LiFePO_4$-based cathode can have significantly better performance characteristics if mixed with $LiCoO_2$, while still costing less than cathodes produced using exclusively $LiCoO_2$.

Acknowledgments

All a data collection was carried out at the Jet Propulsion Laboratory, California Institute of Technology, under contract with the National Aeronautics and Space Administration. Thanks to Marshall Smart for input regarding electrolyte usage.

References

[1] M. Verbrugge, D. Frisch, B. Koch, J. Electrochem. Soc. 152 (2005) A333–A342.
[2] R.N. Mayo, P. Ranganathan, Power-Aware Comput. Syst. 3164 (2004) 26–40.
[3] A.I. Harrison, J. Power Sources 116 (2003) 232–235.
[4] L.T. Lam, R. Louey, J. Power Sources 158 (2006) 1140–1148.
[5] R. Chandrasekaran, G. Sikha, B.N. Popov, J. Appl. Electrochem. 35 (2005) 1005–1013.
[6] J. Han, E.S. Park, J. Power Sources 112 (2002) 477–483.
[7] J. Barker, M. Saudi, K. Yazid, E. Tracy, U.S. Patent 7041239 (2006).
[8] S.H. Park, S.H. Kang, C.S. Johnson, K. Amine, M.M. Thackeray, Electrochem. Commun. 9 (2007) 262–268.
[9] J.C. Arrebola, A. Caballero, L. Hernan, J. Morales, Electrochem. Solid State Lett. 8 (2005) A641–A645.
[10] Z.F. Ma, X.Q. Yang, X.Z. Liao, X. Sun, J. McBreen, Electrochem. Commun. 3 (2001) 425–428.
[11] A.M. Stux, K.E. Swider-Lyons, J. Electrochem. Soc. 152 (2005) A2009–A2016.
[12] N. Imachi, Y. Takano, H. Fujimoto, Y. Kida, S. Fujitani, J. Electrochem. Soc. 154 (2007) A412–A416.
[13] Y.K. Fan, J.M. Wang, Z. Tang, W.C. He, J.Q. Zhang, Electrochim. Acta 52 (2007) 3870–3875.
[14] C.M. Julien, K. Zaghib, A. Mauger, M. Massot, A. Ait-Salah, M. Selmane, F. Gendron, J. Appl. Phys. 100 (2006).
[15] H.W. Chan, J.G. Duh, H.S. Sheu, J. Electrochem. Soc. 153 (2006) A1533–A1538.
[16] Y. Chen, C.-W. Wang, G. Liu, X.-Y. Song, V.S. Battaglia, A.M. Sastry, J. Electrochem. Soc. 154 (2007) A978–A986.
[17] M.M. Thackeray, S.H. Kang, C.S. Johnson, J.T. Vaughey, R. Benedek, S.A. Hackney, J. Mater. Chem. 17 (2007) 3112–3125.
[18] M.M. Thackeray, C.S. Johnson, J.T. Vaughey, N. Li, S.A. Hackney, J. Mater. Chem. 15 (2005) 2257–2267.
[19] Y. Wu, A. Manthiram, Electrochem. Solid State Lett. 9 (2006) A221–A224.
[20] Z.H. Lu, J.R. Dahn, J. Electrochem. Soc. 149 (2002) A815–A822.
[21] Z.H. Lu, L.Y. Beaulieu, R.A. Donaberger, C.L. Thomas, J.R. Dahn, J. Electrochem. Soc. 149 (2002) A778–A791.
[22] Z.H. Lu, D.D. Macneil, J.R. Dahn, Electrochem. Solid State Lett. 4 (2001) A191–A194.
[23] K. Zaghib, A. Mauger, J.B. Goodenough, F. Gendron, C.M. Julien, Chem. Mater. 19 (2007) 3740–3747.
[24] K. Zaghib, P. Charest, A. Guerfi, J. Shim, M. Perrier, K. Striebel, J. Power Sources 134 (2004) 124–129.
[25] Y.J. Park, Y.S. Hong, X.L. Wu, K.S. Ryu, S.H. Chang, J. Power Sources 129 (2004) 288–295.
[26] M. Zhang, L.F. Jiao, H.T. Yuan, Y.M. Wang, J. Guo, M. Zhao, W. Wang, X.D. Zhou, Solid State Ionics 177 (2006) 3309–3314.
[27] M.C. Smart, J.F. Whitacre, B.V. Ratnakumar, K. Amine, J. Power Sources 168 (2007) 501–508.

[28] M.C. Smart, B.V. Ratnakumar, J.F. Whitacre, L.D. Whitcanack, K.B. Chin, M.D. Rodriguez, D. Zhao, S.G. Greenbaum, S. Surampudi, J. Electrochem. Soc. 152 (2005) A1096–A1104.
[29] A.M. Kannan, L. Rabenberg, A. Manthiram, Electrochem. Solid State Lett. 6 (2003) A16–A18.
[30] J. Marzec, W. Ojczyk, J. Molenda, Mater. Sci.-Poland 24 (2006) 69–74.
[31] X.Y. Chang, Z.X. Wang, X.H. Li, L. Zhang, H.J. Guo, W.J. Peng, Mater. Res. Bull. 40 (2005) 1513–1520.
[32] J.F. Whitacre, W.C. West, B.V. Ratnakumar, J. Electrochem. Soc. 150 (2003) A1676–A1683.